Shell-Driven Magnetic Stability in Core-Shell Nanoparticles

J. Nogués,[1,*] V. Skumryev,[1] J. Sort,[1] S. Stoyanov,[2] and D. Givord[3]

[1]*Institució Catalana de Recerca i Estudis Avançats (ICREA) and Departament de Física, Universitat Autònoma de Barcelona, 08193 Bellaterra, Barcelona, Spain*

[2]*Department of Physics and Astronomy, University of Delaware, Newark, Delaware 19716, USA*

[3]*Laboratoire Louis Néel, CNRS-Grenoble, 38042-Grenoble-cedex 9, France*

(Received 13 February 2006; published 13 October 2006)

The magnetic properties of ferromagnetic-antiferromagnetic Co-CoO core-shell nanoparticles are investigated as a function of the in-plane coverage density from 3.5% to 15%. The superparamagnetic blocking temperature, the coercivity, and the bias field radically increase with increasing coverage. This behavior cannot be attributed to the overall interactions between cores. Rather, it can be semiquantitatively understood by assuming that the shells of *isolated* core-shell nanoparticles have strongly degraded magnetic properties, which are rapidly recovered as nanoparticles come into contact.

DOI: 10.1103/PhysRevLett.97.157203 PACS numbers: 75.75.+a, 75.30.Et, 75.50.Ee

Interest in ferromagnetic (FM) nanoparticles has been steadily increasing in recent years catalyzed by their rapidly expanding areas of potential application, ranging from ultrahigh density recording media to medicine [1,2]. Below a certain critical size, FM nanoparticles become superparamagnetic above the blocking temperature, T_B^{SP}. The need for T_B^{SP} to be above room temperature constitutes the superparamagnetic limit in magnetic recording media [3]. Besides this size effect, the nanoparticle behavior is influenced by the proximity of neighboring particles. As the nanoparticle density is progressively increased, dipolar interparticle interactions lead to the appearance of *collective behaviors* [4,5], i.e., the particle moments no longer switch independently [6,7]. Additionally, above a critical density there is a tendency for the nanoparticles to coalesce, forming larger aggregates [8,9].

The existence of correlated magnetic states and the occurrence of clustering are undesirable for recording. To reduce these effects, metallic nanoparticles are commonly protected by a native oxide shell. Although most of the native oxide shells of transition metals (Fe, Co, Ni) are either antiferromagnetic or ferrimagnetic, their magnetic effects on the FM metallic core have either been neglected or reported to be effective only at low temperatures [10,11]. For example, exchange bias [12], typical of FM-AFM coupling, has been usually observed far below room temperature [11,13] and, close to room temperature, the shell has been traditionally claimed to constitute only a barrier against coalescence.

In the present study, core-shell nanoparticles (Co-CoO: FM-AFM) are examined for coverage densities in which dipolar interactions are not expected to dominate the magnetic behavior. The coercivity, the bias field, and the magnetic stability are drastically enhanced as the nanoparticle concentration increases. This unexpected behavior is suggested to originate from the ''recovery'' of the shell magnetic properties when the shells are no longer isolated but come into contact.

The sample growth has been described in detail in Ref. [14]. In short, Co-CoO core-shell nanoparticles, embedded in an Al_2O_3 matrix, were prepared as pseudo-multilayers. The thickness of the Al_2O_3 matrix layers was kept at 15 nm, i.e., large enough to avoid dipolar interactions between the Co-CoO nanoparticle layers. The nanoparticles (core + shell) have an average diameter $\Phi_{\text{core+shell}} = \Phi_{\text{core}} + 2t_{\text{shell}} = 6$ nm, with $t_{\text{shell}} = 1$ nm and $\Phi_{\text{core}} = 4$ nm. Three samples, labeled S_1, S_2, and S_3, corresponding to coverage densities of 3.5%, 5.5%, and 15% in terms of ferromagnetic cores (or 8%, 13%, and 33% in terms of cores + shells) were prepared by controlling the nanoparticle deposition time. A ''fully dense'' sample, which contained no Al_2O_3 matrix layer, labeled S_D, was also grown to serve as a reference.

As seen in Fig. 1, T_B^{SP} [obtained from the maximum in $m_{ZFC}(T)$], which is 5 K for S_1, reaches 220 K for sample S_3. Similarly, the coercive field, H_C, and the exchange bias field, H_E, of field cooled samples are much larger for sample S_3 than for S_1 [see Fig. 2(a) and 2(b)]: at 2 K,

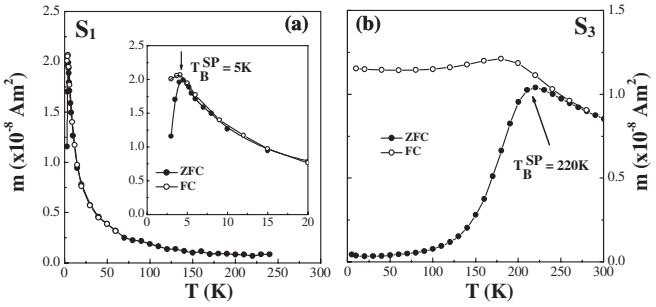

FIG. 1. Temperature dependence of the field cooled FC (m_{FC}—open symbols) and zero field cooled ZFC (m_{ZFC}—filled symbols) magnetization for the (a) S_1 and (b) S_3 samples at $\mu_o H = 5$ mT. Shown in the inset of (a) is a low temperature magnification of the magnetization. The superparamagnetic blocking temperature, T_B^{SP}, is indicated by an arrow. The lines are guides to the eye.

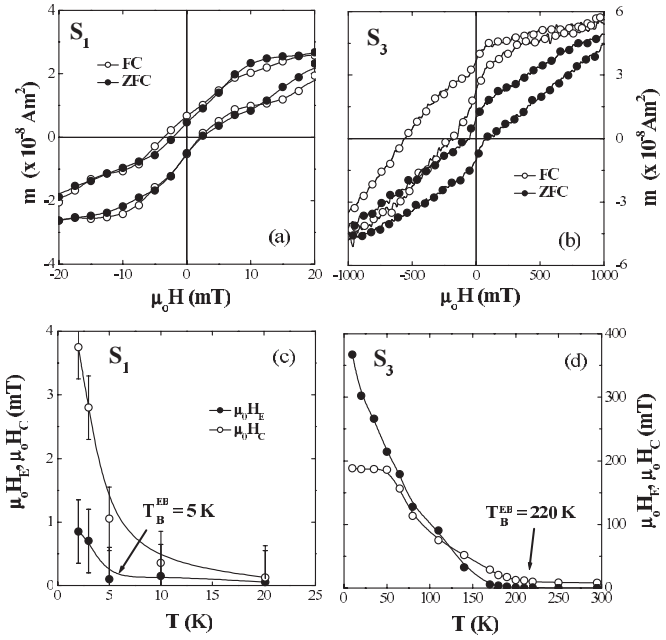

FIG. 2. Field cooled (FC), in $\mu_o H_{\rm FC} = 5$ T, and zero field cooled (ZFC) hysteresis loops for (a) S_1 (at $T = 3$ K) and (b) S_3 (at $T = 10$ K) samples. Temperature dependence of the coercivity, $\mu_o H_C$, and exchange bias, $\mu_o H_E$, for (c) S_1 and (d) S_3 samples. The exchange-bias blocking temperature, $T_B^{\rm EB}$, is indicated by an arrow. The lines are guides to the eye.

$\mu_o H_C = 3.8$ mT and $\mu_o H_E = 0.8$ mT, for sample S_1, while $\mu_o H_C = 187$ mT and $\mu_o H_E = 367$ mT for sample S_3. Correspondingly, the exchange-bias field blocking temperature, $T_B^{\rm EB}$ (i.e., the temperature at which $H_E = 0$ upon heating) raises for increasing density, from $T_B^{\rm EB} \approx 5$ K in S_1 to $T_B^{\rm EB} = 200$ K in S_3 [see Fig. 2(c) and 2(d)]. Altogether, $\mu_o H_C$, $\mu_o H_E$, $T_B^{\rm EB}$, and $T_B^{\rm SP}$ are found to increase considerably with the nanoparticle density [Fig. 3(a) and 3(b)]. This radical dependence of the magnetic behaviors on the nanoparticle coverage indicates that an enhancement in the barrier against reversal occurs as the coverage density is increased, even modestly.

For a nanoparticle with $\Phi_{\rm core} = 4$ nm and anisotropy $K_{\rm Co}({\rm fcc}) = 8 \times 10^4$ J/m^3 the calculated $T_B^{\rm SP} = KV/25k_B$

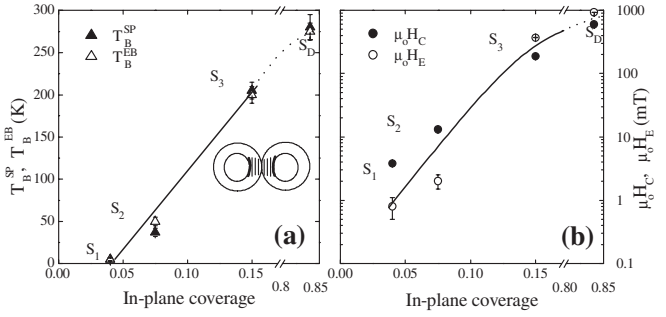

FIG. 3. Dependence of (a) the superparamagnetic and exchange-bias blocking temperatures, $T_B^{\rm SP}$ and $T_B^{\rm EB}$ and (b) the coercivity, $\mu_o H_C$, and exchange bias, $\mu_o H_E$, on the in-plane nanoparticle density. The lines are guides to the eye. Note the break in the x axes.

(where V is the volume) should be about 6 K. This $T_B^{\rm SP}$ value is of the order of magnitude of the experimental $T_B^{\rm SP} = 5$ K in the most diluted sample, S_1.

Classically, the drastic increase in $T_B^{\rm SP}$ and exchange-bias properties would be simply attributed to interparticle dipolar interactions. As the core concentration increases from 3.5% to 15%, and the interparticle dipolar interactions develop, the present system is expected to evolve from the superparamagnetic state to the superspin glass state [6,7]. At such particle concentrations, which are much below the percolation limit [15], comparison with the existing literature indicates that the expected $T_B^{\rm SP}$ is typically below 50 K. In view of obtaining a more quantitative estimate of the expected $T_B^{\rm SP}$, it is meaningful to compare the present data to those obtained for the Co-SiO_2 system by Nunes *et al.* [16]. These authors developed a quantitative phenomenological analysis of the magnetic behavior of nanoparticle assemblies, which is derived from the well-known random anisotropy model [17]. Scaling their results to the particle size and densities of the present Co-CoO system leads to a predicted $T_B^{\rm SP}$ which increases from 5 K in S_1 to 35 K in sample S_3. Such $T_B^{\rm SP}$ values are close to those derived theoretically from Monte-Carlo simulations [18]; however, they are much weaker than the experimental $T_B^{\rm SP}$ values. It can thus be concluded that dipolar interactions cannot constitute the main cause for the observed increase in $T_B^{\rm SP}$.

Similarly, considering the extremely short-range character of exchange interactions and the fact that the cores are isolated by at least twice the shell thickness, the possible coupling of Co cores through such interactions can also be ruled out.

Since neither dipolar interactions nor exchange interactions can be invoked, we are led to consider the possible influence of the CoO shell in stabilizing the core moments. In Refs. [14,19] we showed that the Co FM cores were stabilized by interactions with an AFM CoO matrix. In particular, the derived energy barrier, using $K_{\rm CoO} = 2.7 \times 10^7$ J/m^3 [20], becomes $\Delta E = 0.17 \times 10^{-2}$ J/m^2 [14,19], which under the usual assumption that $\Delta E = 25 k_B T_B^{\rm SP}$, leads to $T_B^{\rm SP} = 290$ K.

In this analysis it is implicitly assumed that the CoO moments are fixed and not thermally activated. This is justified since, due to the very strong anisotropy of CoO, 1 nm thick CoO shells should be stable up to their Néel temperature, $T_N({\rm CoO}) = 290$ K (namely, $K_{\rm CoO} V_{\rm shell}/25k_B \gg T_N$). Consequently, core-shell coupling should stabilize the Co FM core moment for an *isolated* Co-CoO nanoparticle as it does for a Co nanoparticle embedded in a continuous CoO matrix [14]. This disagrees with experimental observations, suggesting that the magnetic properties of the AFM CoO shell differ from the properties of bulk CoO.

The proposed degradation of the CoO shell magnetic properties at small thickness is reminiscent to the well-known fact that in CoO thin films the ordering temperature decreases drastically below 1 nm [21] and the CoO anisot-

ropy is concomitantly reduced. Similar effects are observed in CoO nanoparticles [22,23]. In the present case, t_{shell} is precisely in the range where the drop in the CoO T_N occurs. The value of T_N constitutes an upper limit for that of T_B^{SP} (shell). Consequently the CoO shell covering an *isolated* Co-CoO nanoparticle cannot induce the huge increase in T_B^{SP} (core) occurring for Co nanoparticles embedded in a CoO matrix.

As the nanoparticle concentration is increased, shells may come into contact and, when this occurs, the CoO thickness is expected to be *locally* increased to about 2 nm [see inset in Fig. 3(a)]. When this happens, the CoO bulk antiferromagnetic properties and thus the interfacial coupling are expected to be *locally* recovered. Consequently, an increase in the blocking temperature, ΔT_B^{SP}, will occur. Note that when AFM oxide nanoparticles come into contact, the magnetic correlation is known to increase [24]. Moreover, isolated Co-CoO core-shell nanoparticles with $t_{shell} \sim 3.2$ nm have been reported to exhibit moderate exchange bias and to be stable up to 170 K, while when $t_{shell} \sim 1$ nm no exchange bias has been observed [25].

To reach a more quantitative understanding of this effect, we assume that, for a given particle, the recovered area and the associated increase in the blocking temperature are proportional to the number of particles, n_c, which are in contact with it. Denoting β the recovered fraction resulting from the contact between two particles, the total recovered fraction amounts to $n_c\beta$ with the condition $n_c\beta \leq 1$. Thus, $\Delta T_B^{SP}(n_c) = n_c\beta 290$ (K). In view of applying the model to nanoparticle assemblies, the probability that a given nanoparticle is in contact with n_c other nanoparticles has been evaluated by modeling the system as a 2D random packing of hard spheres, following Philipse's model [26]. The positions of the spheres in the Philipse's model constitute sites, of which the occupancy probability p is equal to n_p/N_T, where n_p is the experimental core + shell in-plane coverage density—e.g., 0.29×10^{16} particles/m^2 for S_3—and N_T is the density of available sites (taking into account that 0.84 is the maximum possible density), which amounts to 0.74×10^{16} particles/m^2 for 6 nm spheres. The occupancy probability ranges from $p = 0.1$ (S_1) to $p = 0.39$ (S_3). Moreover, to take into account that the coverage is only partial and hence the spheres do not interfere strongly, the maximum number of nearest neighbor spheres was taken as 4, rather than 3.35 as in Philipse's model. The probability, $P(n_c)$, for a given nanoparticle to be in contact with n_c ($n_c = 0$ to 4) neighboring nanoparticles is then given by simple statistics (Table I). For S_1 ($p = 0.1$) and S_2 ($p = 0.15$), most of the nanoparticles are isolated. However, for S_3 ($p = 0.39$), the number of nanoparticles with one or more neighbors becomes larger than the number of isolated particles.

In view of comparing these calculations to experimental results, a single layer sample, adequate for TEM analysis, was prepared with an expected in-plane particle density identical to S_1. Over a surface area of 1.55×10^5 nm^2, 147 particles were found, including 4 couples and 1 triplet. This corresponds to $11/147 = 7.5$ (2.8)% of the particles not being isolated. Within statistical error, this agrees with the value 11% that would be expected from statistics within the Phillipse's model.

It may be thought that the $\Delta T_B^{SP}(n_c)$ values in the present samples may be deduced directly from the $P(n_c)$ values listed in Table I. However, in order to describe the blocking of the moments for such nanoparticle assemblies, the dipolar interactions created by the fraction of blocked particles on otherwise superparamagnetic particles in contact with them must be considered in addition to the pure thermal activation effects. Assuming simple dipolar interactions, the magnetic field, B_{block}, created by a blocked particle on the n_c neighboring particles, is evaluated to be 0.042 T. Considering that the particle magnetic moment amounts to $5300\mu_B$, this is equivalent to 150 K. Hence, the associated value of the parameter x in the Langevin or Brillouin function of the superparamagnetic particle is close to 1 for the present experimental conditions; consequently, the particle moment becomes substantially magnetized under the effect of this field [27]. This implies that a superparamagnetic nanoparticle in contact with a blocked one will become polarized under the effect of the dipolar field of the later one [27] (note that this is not rigorously true for $T = 290$ K, but is of no importance for the present discussion since the highest considered blocking temperature amounts to 200 K). This polarization effect will propagate further to next neighbors, but due to incomplete magnetization it will be damped rapidly. This effect may be described as dipolar-enhanced blocking.

As it becomes clear from the experimental data, $\Delta T_B^{SP}(n_c)$ may be semiquantitatively explained when it is assumed that the magnetic properties are fully recovered for particles for which $n_c = 4$. This implies that $\beta = 0.25$. With this β value, $\Delta T_B^{SP}(n_c)$ for a given nanoparticle amounts to 72 K, 150 K, 215 K, and 285 K for $n_c = 1$, 2, 3, and 4, respectively, (the associated T_B^{SP} values are 5 K higher). In S_3, the moments of the 2.3% fraction of $n_c = 4$ particles freeze at 290 K. The number of particles which become polarized at 290 K under the effect of B_{block} amounts approximately to $3.85 \times 2.3\% = 8.9\%$ [28]. Similarly, the moments of the 14.5% fraction of particles with 3 neighbors freeze at 220 K and $2 \times 14.5\% = 29\%$ [28] become magnetized at 220 K under B_{block}. Thus, an additional 44% of the particles become blocked at this

TABLE I. Probability $P(n_c)$ for a given particle to be in contact with n_c ($n_c = 0$–4) other particles

	$P(n_c)$				
Sample	0	1	2	3	4
S_1 ($p = 0.1$)	0.656	0.292	0.049	0.004	0
S_2 ($p = 0.15$)	0.520	0.368	0.098	0.012	0.001
S_3 ($p = 0.39$)	0.140	0.354	0.340	0.145	0.023

temperature. The actual value should be slightly higher due to the next-nearest-neighbors extension of the polarization. Hence, the blocking of the $n_c = 3$ particles determines the experimental value of T_B^{SP} in this sample at $T_B^{SP} = 220$ K. Applying this approach to S_2 leads to $T_B^{SP} = 77$ K. For S_1, since most of the particles are isolated and considering the strong susceptibility increase at low temperature, the expected T_B^{SP} would be $T_B^{SP} = 5$ K.

Although this model presents a first order approximation to the present phenomenon and, in particular, dipolar interactions are neglected between particles which are not in direct contact, the experimental T_B^{SP} values are in rather good agreement with the values predicted. Moreover, this model also explains the unusual shape of the hysteresis loops (i.e., constricted loops around $H = 0$) observed experimentally [Fig. 2(a) and 2(b)], which can be ascribed to the nanoparticles with no neighbors that should remain superparamagnetic down to low temperatures. Note that for the fully dense sample, since all the nanoparticles are surrounded by several other nanoparticles, no constriction in the loop is observed [14]. Other effects such as the scatter in T_B^{SP}, $\mu_o H_E$, and $\mu_o H_C$ values found in the literature [11,13,14,19,25,29–39] could also be accounted for. Although part of the spread in results arises from the diverse Φ_{core} and t_{shell}, distinctive growth methods should render dissimilar packing of the nanoparticles, which, according to the above discussion, should result in a range of values for T_B^{SP}, $\mu_o H_E$, and $\mu_o H_C$.

In conclusion, we have demonstrated that the magnetic properties of FM-AFM core-shell (Co-CoO) nanoparticles depend strongly on the in-plane coverage, even in the diluted regime (less than 25% coverage in terms of ferromagnetic cores). This small increase in in-plane density brings about a 40-fold, 50-fold, and 400-fold increase in T_B^{SP}, $\mu_o H_C$, and $\mu_o H_E$, respectively. The reported results demonstrate the essential role played by the shells in stabilizing the magnetism of core-shell nanoparticles. Actually, shell mediated interactions may hold the key for the applicability of future recording media based on single nanoparticles protected by either a native oxide [10] or artificial shells [40,41], due to induced correlated magnetic states.

We wish to thank G. Hadjipanayis for his support, Y. Zhang for his help in TEM imaging, and N. M. Dempsey for critical reading of the manuscript. This work was supported by the Spanish CICYT (No. MAT2004-01679) and the Catalan DGR (No. 2005SGR00401).

*Email address: Josep.Nogues@uab.es

[1] M. A. Willard *et al.*, Int. Mater. Rev. **49**, 125 (2004); T. Hyeon, Chem. Commun. (Cambridge) 08 (2003) 927; S. P. Gubin, Y. A. Koksharov, G. B. Khomutov, and G. Y. Yurkov, Russian Chemical Reviews **74**, 489 (2005); P. Tartaj *et al.*, J. Phys. D **36**, R182 (2003).
[2] R. H. Kodama, J. Magn. Magn. Mater. **200**, 359 (1999); X. Batlle and A. Labarta, J. Phys. D **35**, R15 (2002); W. Wernsdorfer, Adv. Chem. Phys. **118**, 99 (2001); J. L. Dormann, D. Fiorani, and E. Tronc, Adv. Chem. Phys. **98**, 283 (1997).
[3] D. Weller and A. Moser, IEEE Trans. Magn. **35**, 4423 (1999).
[4] J. F. Löffler, H. B. Braun, and W. Wagner, Phys. Rev. Lett. **85**, 1990 (2000).
[5] V. F. Puntes *et al.*, Nat. Mater. **3**, 263 (2004).
[6] X. Chen *et al.*, Phys. Rev. B **70**, 172411 (2004).
[7] P. Allia *et al.*, Phys. Rev. B **64**, 144420 (2001).
[8] S. Sankar, A. E. Berkowitz, and D. J. Smith, Phys. Rev. B **62**, 14 273 (2000).
[9] S. Yamamuro *et al.*, Mater. Trans. JIM **40**, 1450 (1999).
[10] M. P. Sharrock, IEEE Trans. Magn. **36**, 2420 (2000).
[11] J. Nogués *et al.*, Phys. Rep. **422**, 65 (2005).
[12] J. Nogués and I. K. Schuller, J. Magn. Magn. Mater. **192**, 203 (1999).
[13] J. Nogués *et al.*, Int. J. Nanotechnol. **2**, 23 (2005).
[14] V. Skumryev *et al.*, Nature (London) **423**, 850 (2003).
[15] C. L. Chien, J. Appl. Phys. **69**, 5267 (1991).
[16] W. C. Nunes *et al.*, Phys. Rev. B **72**, 212413 (2005).
[17] J. Löffler *et al.*, Phys. Rev. B **57**, 2915 (1998).
[18] M. Bahiana *et al.*, J. Magn. Magn. Mater. **281**, 372 (2004).
[19] D. Givord, V. Skumryev, and J. Nogués, J. Magn. Magn. Mater. **294**, 111 (2005).
[20] J. Kanamori, Prog. Theor. Phys. **17**, 177 (1957).
[21] Y. J. Tang *et al.*, Phys. Rev. B **67**, 054408 (2003).
[22] L. Wang *et al.*, Chem. Mater. **16**, 5394 (2004).
[23] S. Sako *et al.*, Surf. Rev. Lett. **3**, 109 (1996).
[24] C. Frandsen *et al.*, Phys. Rev. B **72**, 214406 (2005).
[25] J. B. Tracy *et al.*, Phys. Rev. B **72**, 064404 (2005).
[26] A. P. Philipse, Colloids Surf. A **213**, 167 (2003).
[27] O. Fruchart *et al.*, J. Magn. Magn. Mater. **239**, 224 (2002).
[28] The coefficients 3.85 and 2, instead of 4 and 3, respectively, are obtained when statistical account is taken of the possible occurrence of (i) various types of environments and of (ii) larger aggregates encompassing 2nd and 3rd nearest neighbors.
[29] W. H. Meiklejohn and C. P. Bean, Phys. Rev. **102**, 1413 (1956).
[30] R. Morel, A. Brenac, and C. Portemont, J. Appl. Phys. **95**, 3757 (2004); C. Portemont *et al.*, J. Appl. Phys. **100**, 033907 (2006).
[31] D. L. Peng *et al.*, Phys. Rev. B **60**, 2093 (1999).
[32] C. Luna *et al.*, Nanotechnology **15**, S293 (2004).
[33] A. N. Dobrynin *et al.*, Appl. Phys. Lett. **87**, 012501 (2005).
[34] O. Iglesias, X. Batlle, and A. Labarta, Phys. Rev. B **72**, 212401 (2005).
[35] J. M. Riveiro *et al.*, Appl. Phys. Lett. **86**, 172503 (2005).
[36] J. A. De Toro *et al.*, Phys. Rev. B **73**, 094449 (2006).
[37] M. Spasova *et al.*, J. Magn. Magn. Mater. **272**, 1508 (2004).
[38] H. Bi *et al.*, Phys. Lett. A **307**, 69 (2003).
[39] S. Gangopadhyay *et al.*, IEEE Trans. Magn. **29**, 2619 (1993).
[40] H. Zeng *et al.*, Nano Lett. **4**, 187 (2004).
[41] C. Liu *et al.*, Chem. Mater. **17**, 620 (2005).